BIOCHEMISTRY
including biophysical chemistry & molecular biology
Article

Biochemistry **2010,** *49,* 2235–2245 2235
DOI: 10.1021/bi902085q

Mutational Analysis of Threonine 402 Adjacent to the GXXXG Dimerization Motif in Transmembrane Segment 1 of ABCG2[†]

Orsolya Polgar,[‡,#] Caterina Ierano,[‡,#] Akina Tamaki,[‡] Bradford Stanley,[∥] Yvona Ward,[@] Di Xia,[§] Nadya Tarasova,[⊥] Robert W. Robey,[‡] and Susan E. Bates*[,‡]

[‡]*Medical Oncology Branch, and* [§]*Laboratory of Cell Biology, Center for Cancer Research, National Cancer Institute, National Institutes of Health, 9000 Rockville Pike, Building 10, Room 13N240, Bethesda, Maryland 20892,* [∥]*Department of Molecular Biophysics and Biochemistry, Yale University, New Haven, Connecticut 06520,* [⊥]*Molecular Aspects of Drug Design Section, Structural Biophysics Laboratory, NCI-Frederick, Building 538-FCRDC, Room 165, Fort Detrick, Frederick, Maryland 21702, and* [@]*Cell and Cancer Biology Branch, Center for Cancer Research, National Cancer Institute, National Institutes of Health, 9000 Rockville Pike, Building 10, Room 3B43, Bethesda, Maryland 20892* [#]*These authors contributed equally to this work.*

Received December 4, 2009

ABSTRACT: ABCG2 is an ATP-binding cassette half-transporter important in normal tissue protection, drug distribution, and excretion. ABCG2 requires homodimerization for function, though the mechanism for dimerization has not been elucidated. We conducted mutational analysis of threonine 402, three residues from the GXXXG motif in TM1, to study its potential role in ABCG2 dimerization (TXXXGXXXG). Single mutations to leucine (T402L) or arginine (T402R) did not have a significant impact on the ABCG2 protein. On the other hand, combining the T402 mutations with the GXXXG glycine to leucine mutations (T402L/G406L/G410L and T402R/G406L/G410L) resulted in a substantially reduced level of expression, altered glycosylation, degradation by a proteosome-independent pathway, and partial retention in the endoplasmic reticulum as suggested by immunostaining, Endo H sensitivity, and MG132 and bafilomycin failed effect. The T402L/G406L/G410L mutant when incubated with the ABCG2 substrate MX showed a shift on immunoblot analysis to the band representing the fully mature glycoprotein. The T402R/G406L/G410L mutant carrying the more drastic substitution was found to primarily localize intracellularly. The same set of mutations also displayed impaired dimerization in the TOXCAT assay for TM1 compared to that of the wild type. Homology modeling of ABCG2 places the TXXXGXXXG motif at the dimer interface. These studies are consistent with a role for the extended TXXXGXXXG motif in ABCG2 folding, processing, and/or dimerization.

ABCG2 is a member of the G subfamily of human ATP-binding cassette (ABC)[1] transporters (*1*). It was first described approximately a decade ago in multidrug-resistant cancer cell lines that did not overexpress the previously known multidrug ABC transporters Pgp and MRP1 (*2*−*4*). Accordingly, the first of its substrates identified were chemotherapeutic agents, such as topotecan, daunorubicin, methotrexate, SN-38, and flavopiridol (*4*−*8*). Subsequently, a rapidly growing number of substrates and inhibitors representing various chemical and pharmacological groups have been described (*9*). ABCG2 is also suggested to play an important protective role in the blood−brain and maternal−fetal barriers (*10*), and upon characterization of its SNPs, a significant role in the pharmacogenomics and pharmacokinetics of its substrates has emerged (*11*). Most recently, ABCG2 has received significant attention as a marker of hematopoetic stem cells (*12*).

Despite intensive research efforts, our knowledge of the structure of ABCG2 is currently quite limited. Determining the three-dimensional structure would be valuable in understanding structure−function relationships and designing modulators of the transporter with potential clinical benefit either in overcoming multidrug resistance in cancer or as part of individualized therapy for people carrying SNPs with functional consequences. ABCG2 is considered a half-transporter, and while it is well established that it must homodimerize for normal function, the process of dimerization is not yet fully understood. Disulfide bonds between the monomers have been suggested to play a key role in ABCG2 dimerization, and one such bond between cysteine 603 residues localized in the extracellular loop connecting TM5 and TM6 is characterized in the literature (*13*, *14*). In contrast, cysteines 592 and 608 in the same loop were suggested to form intramolecular disulfide bonds within the monomer (*13*, *15*). Most recently, all

[†]This research was supported by the Intramural Research Program of the National Institutes of Health, National Cancer Institute, Center for Cancer Research.

*To whom correspondence should be addressed. E-mail: sebates@helix.nih.gov. Telephone: (301) 402-1357. Fax: (301) 402-1608.

[1]Abbreviations: ABC, ATP-binding cassette; TM, transmembrane segment; SNP, single-nucleotide polymorphism; MRP1, multidrug resistance-associated protein 1; GAPDH, glyceraldehyde 3-phosphate dehydrogenase; ER, endoplasmic reticulum; DSS, disuccinimidyl suberate; DSG, disuccinimidyl glutarate; MBP, maltose binding protein; SDS−PAGE, sodium dodecyl sulfate−polyacrylamide gel electrophoresis; PCR, polymerase chain reaction; Endo H, endoglycosidase H; HEK, human embryonic kidney; FTC, fumitremorgin C; MX, mitoxantrone; Pgp, P-glycoprotein; CFTR, cystic fibrosis transmembrane conductance regulator; CAT, chloramphenicol acetyltransferase; PVDF, polyvinylidene fluoride; NBD, nucleotide binding domain; TMD, transmembrane domain; LIPS, lipid-facing surface; PDB, Protein Data Bank; ERAD, ER-associated degradation system; GPCR, G-protein-coupled receptor.

© 2010 American Chemical Society
Published on Web 01/20/2010

three of these cysteines were shown to engage in intermolecular disulfide bonding (*16*). Nevertheless, when either cysteine 603 or all three of these cysteines are substituted, the protein retains its function (*13*, *14*, *16*), implying that disulfide bond formation cannot be the sole or even principal force keeping the monomers together. Note that this is also true for the homodimerizing bacterial ABC transporter LmrA, which does not contain any cysteine residues (*17*), and for the heterodimerizing human ABC half-transporters TAP1 and TAP2, the cysteine-less mutants of which are fully functional (*18*).

In a previous study, we reported mutational analysis of the GXXXG putative dimerization motif in TM1 of the ABCG2 protein (*19*). The GXXXG motif (two glycines separated by any three amino acids) has been shown to mediate packing of transmembrane α-helices by permitting close association and thus allowing interactions between the helix backbones and also between the side chains of surrounding residues (*20*). Its role has most extensively been studied in glycophorin A, a major sialoglycoprotein of the red blood cell membrane that comprises one of the blood group antigens. This single-transmembrane helix protein forms a homodimer in which the GXXXG motif plays a critical role (*21*). We found that mutating both glycines of the GXXXG motif to leucines renders the ABCG2 protein inactive, but it retains its ability to traffic to the cell surface. On the other hand, replacing the glycines with alanines, thus creating a putative alternative dimerization motif, AXXXA, results in a fully functional transporter. In glycophorin A, an extended sequence surrounding the GXXXG motif has been shown to be essential for proper dimerization (LIXXGVXXGVXXT). The threonine in this motif is suggested to stabilize the dimer by forming a hydrogen bond (*22*). Notably, ABCG2 also has a threonine separated by three residues from its GXXXG motif. In both cases, the threonine is located on the cytoplasmic side of the GXXXG motif. Here, we report studies aimed at evaluating the role of this threonine residue in dimer formation in ABCG2 by substitution with the nonpolar leucine and the positively charged arginine.

EXPERIMENTAL PROCEDURES

Cell Culture. HEK 293 cells (ATCC, Manassas, VA) were cultured in Minimal Essential Medium (Invitrogen, Carlsbad, CA), supplemented with 10% fetal bovine serum (Invitrogen), 2 mM glutamine, and 100 units/L penicillin/streptomycin at 37 °C in 5% CO_2. Stably transfected cell lines were maintained in 2 mg/mL G418 (Invitrogen).

For the "processing" experiments, cells were incubated overnight at 37 °C with 5 μM MX (Sigma, St. Louis, MO), 3 μM MG132 (Calbiochem, San Diego, CA), or 10 nM bafilomycin (Sigma) followed by protein extraction and immunoblotting as described below.

Mutagenesis and Transfection. The T402L, T402R, T402L/G406L/G410L, and T402R/G406L/G410L mutants were generated by site-directed mutagenesis in the pcDNA3.1/Myc-HisA(−) vector (Invitrogen) as previously described (*19*). The mutations were confirmed by sequencing the plasmids initially, followed by genomic DNA sequencing of one representative clone of each stably transfected mutant cell line for the full-length *ABCG2* insert. The R482G control and G406L/G410L mutant were previously generated and characterized (*19*, *23*).

Stable transfectants were generated in HEK 293 cells as previously described (*19*). Transfections were performed using TransFast transfection reagent (Promega, Madison, WI). Colonies were selected in 2 mg/mL G418 with frequent removal of dead cells and were expanded prior to study.

Protein Extraction and Immunoblot Analysis. Cells were scraped into cold PBS followed by centrifugation at 1200 rpm for 10 min at 4 °C. The cell pellet was then resuspended in cold lysis buffer [5 mM EGTA, 5 mM EDTA, 10 mM Tris (pH 7.4), 10 mM HEPES, 2 mM dithiothreitol (DTT), and 1% Triton X-100] to which 5 μg/mL aprotinin, 5 μg/mL leupeptin, and 2 mM PMSF were added. After 10 min on ice, unlysed cells and nuclei were pelleted at 1200 rpm for 15 min at 4 °C. The protein concentration of the supernatant was determined by the Bradford method with Bio-Rad's Protein Assay Reagent (Bio-Rad, Hercules, CA) compared to BSA standards (Pierce, Rockford, IL).

Immunoblotting was performed as previously described (*19*). Briefly, protein samples were loaded onto precast 7.5% (w/v) SDS−polyacrylamide gels (Bio-Rad), subjected to electrophoresis, and electrotransferred onto PVDF membranes (Millipore, Bedford, MA). Blots were probed with a 1:200 dilution of mouse monoclonal anti-ABCG2 antibody BXP-21 (Kamiya Biomedical, Seattle, WA) and a 1:3000 dilution of the mouse monoclonal anti-GAPDH antibody (American Research Products, Belmont, MA) and visualized with the Odyssey System (LI-COR, Lincoln, NE) using a 1:4000 dilution of the IRDye 800CW goat anti-mouse secondary antibody (LI-COR). Membranes were stained with 0.1% Ponceau S (Sigma) and checked for comparable loading.

For enzymatic deglycosylation, the Glyko N-Glycanase and Glyko Endoglycosidase H kits were used (ProZyme, San Leandro, CA) following the manufacturer's instructions. Cell lysates containing 100−200 μg of protein were incubated with 2 μL of *N*-glycosidase F or 2 μL of Endo H at 37 °C for 3 h followed by immunoblotting as described above.

Flow Cytometry. Flow cytometry with anti-ABCG2 antibody 5D3 (eBioscience, San Diego, CA) was performed as previously described (*19*). Briefly, cells were trypsinized and resuspended in DPBS with 2% bovine serum albumin (BSA) to which phycoerythrin-conjugated 5D3 or phycoerythrin-conjugated mouse IgG2b was added for 30 min. For the transport studies, cells were trypsinized, resuspended in complete medium (phenol red-free IMEM with 10% fetal calf serum) containing 20 μM MX (Sigma), 1 μM pheophorbide a (Frontier Scientific, Logan, UT), or 200 nM BODIPY-prazosin (Invitrogen) with or without the ABCG2 blocker, Fumitremorgin C (FTC), at 10 μM, and incubated for 30 min at 37 °C in 5% CO_2 (FTC was synthesized by T. McCloud, Developmental Therapeutics Program, Natural Products Extraction Laboratory, National Institutes of Health, Bethesda, MD). Cells were then incubated for 1 h at 37 °C in substrate-free medium, continuing with or without 10 μM FTC, and analyzed on a FACSort flow cytometer equipped with both a 488 nm argon laser and a 635 nm red diode laser.

Immunofluorescence. Immunofluorescence studies were performed as previously described (*19*, *24*). Briefly, cells were cultured for 2 days followed by fixation with 4% paraformaldehyde and permeabilization with prechilled (−20 °C) methanol. After being blocked in a buffer containing 2 mg/mL BSA and 20% goat serum, samples were incubated with a 1:100 dilution of the mouse monoclonal anti-ABCG2 antibody, BXP-21 (Kamiya Biomedical), for 2 h at room temperature followed by incubation with the rhodamine-conjugated goat anti-mouse secondary antibody (Jackson ImmunoResearch Laboratories, West Grove, PA). Following three washes with PBS, stained specimens were

mounted on slides and observed on a Zeiss Axio Observer Z1 microscope equipped with a 63×/1.4 oil DIC objective. Confocal images were generated on a Zeiss LSM510 META laser scanning microscope.

Cross-Linking Studies. Chemical cross-linking was performed in vivo on intact cells. After incubation for 30 min at either room temperature or 4 °C with the cross-linking agent DSG (Pierce) or DSS (Pierce) (data not shown) at a final concentration of 2 mM, the reaction was terminated by addition of Tris-HCl (pH 8) to a final concentration of 20 mM, and cells were immediately harvested as described above.

TOXCAT Assay. The homo-oligomerization of ABCG2 TM1 was assessed using the TOXCAT assay as described previously (*25*). Briefly, the TM of interest is expressed as a fusion between MBP and ToxR in MalE deficient/*Escherichia coli*/NT326. MBP ensures proper orientation in the membrane, while ToxR is a dimerization-dependent transcriptional activator. Upon oligomerization of the transmembrane domains under study, the transcription of reporter gene CAT is turned on proportionally to the strength of the transmembrane domain oligomerization. The ABCG2 transmembrane helix 1 sequence (394-ASIAQIIVTVVLGLVIGAIYFGL-416) and its mutants were assayed for oligomerization as described previously (*25*).

Molecular Modeling. A detailed description of the modeling procedures will be published elsewhere. Briefly, the NBD and TMD of ABCG2 were modeled separately and integrated afterward. The first step was to align sequences of ABCG2 and its homologues for the NBD and TMD, respectively. The TMs were predicted on the basis of a consensus approach (*26*), and each TM was refined to ensure a correct membrane orientation using LIPS score calculation (*27*). The crystal structure of bacterial half-ABC transporter Sav1866 was used as the modeling template (PDB entry 2HYD) (*28*). The NBD model was built on the basis of the crystal structure of NBD from *E. coli* maltose transporter MalK (PDB entry 1Q12) (*26*, *29*), which is most identical in sequence to ABCG2.

RESULTS

Threonine 402 Mutants. The most frequently studied model of membrane protein dimerization is the glycophorin A homodimer in which a seven-residue sequence, including a GXXXG motif and a threonine three residues from the GXXXG motif, is required for proper association (*21*). TM1 of ABCG2 also has a threonine separated by three residues from its GXXXG motif. To study the potential role of this threonine in ABCG2 dimerization, we performed substitutions with a leucine (T402L) or arginine (T402R) substitution or combined these substitutions with the glycine to leucine mutations at the GXXXG motif (T402L/G406L/G410L and T402R/G406L/G410L) followed by stable transfections in HEK 293 cells. The T402L mutation was designed to probe the perceived involvement of this residue in hydrogen bonding. We expected the T402R substitution to be a more drastic substitution on the basis of the change in both size and polarity. We used the previously generated G406L/G410L and R482G transfectants in HEK 293 cells as controls (*19*). The R482G mutation is considered a gain-of-function mutation, which enables the protein to transport a wider range of substrates (*23*). As in the previous study (*19*), all the GXXXG and threonine 402 mutants described here carry the R482G mutation. We previously obtained identical results in studies of the GXXXG motif in the wild-type protein (unpublished observation).

Protein Expression and ABCG2 Substrate Transport. Figure 1A demonstrates protein expression levels for one representative clone of each mutant on an immunoblot with the BXP-21 mouse monoclonal anti-ABCG2 antibody. The T402L and T402R mutants exhibited levels comparable to the control (R482G), while the double (G406L/G410L) and triple mutants (T402L/G406L/G410L and T402R/G406L/G410L) had significantly decreased levels. Both double and triple mutants were characterized by a double band, one at the expected 72 kDa level normally observed for ABCG2 on the immunoblot and one at a slightly lower level. In the case of T402R/G406L/G410L, the lower band comprised the majority of the detected protein.

To study the surface expression levels and function of the mutant proteins, flow cytometry was performed on the stably transfected HEK cells. First, cell surface expression was assessed in nonpermeabilized cells using the 5D3 mouse monoclonal anti-ABCG2 antibody, which recognizes an as yet undetermined extracellular epitope of the protein. As shown in the first column of Figure 1B, the control (R482G) and the T402L and T402R mutants displayed similar levels of surface expression. The G406L/G410L and T402L/G406L/G410L mutants displayed substantially lower surface expression levels with the 5D3 antibody. In the T402R/G406L/G410L triple mutant, only a slight shift between the negative control (solid line) and the 5D3-labeled histograms (dashed line) was present. This experiment was performed multiple times, and the results for the clones shown in Figure 1B varied from no detectable levels to the small shift shown in the figure. Two other clones of the same mutant were also tested and similar results observed (data not shown). The mutants were then tested for their ability to transport known ABCG2 substrates. In these experiments (Figure 1B, second, third, and fourth columns), cells were incubated with the substrates in the presence (dashed line) or absence (solid line) of the ABCG2-specific inhibitor FTC. Transport is indicated by a shift to a higher intracellular fluorescence of the drugs when ABCG2 is blocked by the inhibitor. The control and the T402L and T402R mutants were able to efflux MX, pheophorbide a, and BODIDY-prazosin from the cells. As previously observed, no transport in the GXXXG double leucine mutants was observed despite surface expression (*19*). No transport function was observed for the triple mutants for any of the studied substrates, with no shift between the FTC-treated and nontreated histograms. This was an expected result, given the low levels of expression and the fact that the GXXXG double leucine mutant (G406L/G410L) displayed almost no transport activity (*19*).

N-Glycosidase F and Endoglycosidase H Sensitivity. The results of the immunoblot analysis (Figure 1A) suggested that the lower-molecular mass band might correspond to mutant proteins with altered glycosylation retained in the ER, as we observed in previous studies of mutations at G553 and R383 (*24*, *30*). To prove this, we subjected lysates to enzymatic deglycosylation with *N*-glycosidase F and Endo H. As shown in Figure 2A, a lower-molecular mass band was observed in the control (R482G) following digestion with *N*-glycosidase F to remove all N-linked glycans, consistent with removal of the polysaccharide chain from asparagine 596 of ABCG2 as shown following site-directed mutagenesis of N596 (*31*). As expected, no change in molecular mass was observed in the control, T402L, or T402R after Endo H digestion (Figure 2A), since Endo H resistance is consistent with a fully mature glycoprotein. In the double and triple mutants, the higher-molecular mass band appears to be fully processed as it is not sensitive to Endo H. However, the lower-molecular mass band

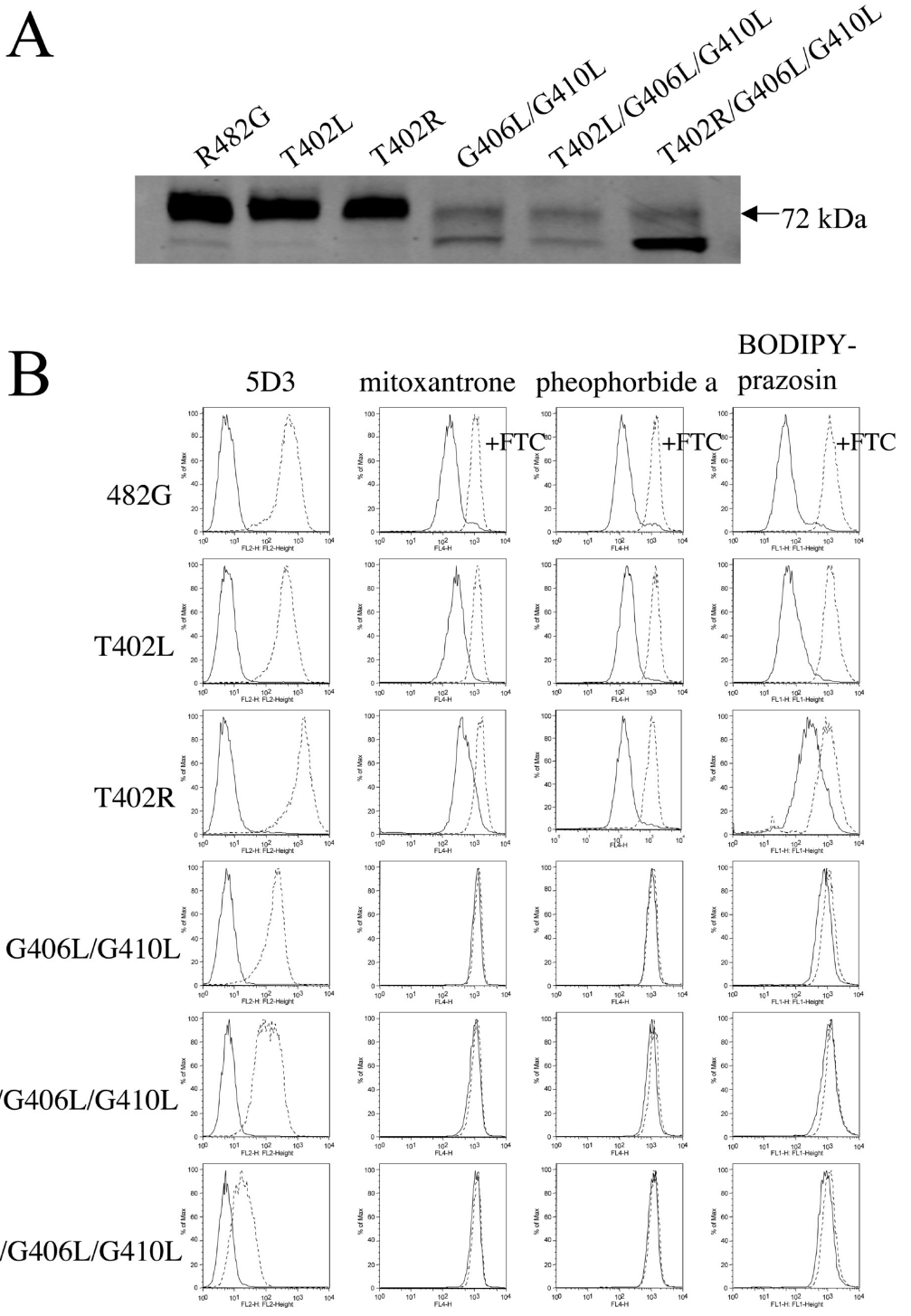

FIGURE 1: Protein levels, surface expression, and function of the mutants. (A) Cell lysates from stably transfected HEK 293 cells (20 μg for R482G, T402L, and T402R and 60 μg for G406L/G410L, T402L/G406L/G410L, and T402R/G406L/G410L) were separated via SDS−PAGE, transferred onto a PVDF membrane, and probed with monoclonal anti-ABCG2 antibody BXP-21. (B) The first column shows the results of flow cytometry with the 5D3 surface antibody. Stably transfected HEK 293 cells were incubated for 30 min in phycoerythrin-labeled negative control antibody (solid line) or 5D3 antibody (dashed line) and analyzed on a FACSsort flow cytometer. For the second, third, and fourth colums, cells were incubated for 30 min in complete medium containing 20 μM MX, 1 μM pheophorbide a, and 200 nM BODIPY-prazosin with or without 10 μM ABCG2 blocker FTC, respectively [accumulation without FTC (solid line) and with FTC (dashed line)].

is sensitive to Endo H in the same mutants. Following either *N*-glycosidase F or Endo H digestion, the triple mutants exhibited the same molecular mass. Minimal change was observed in the molecular mass of ABCG2 in the G406L/G410L mutant after Endo H digestion. The Endo H sensitivity observed in the lower-molecular mass forms suggests that their glycans are immature and proteins have not completed processing in the ER (Figure 2B).

MG132 and Bafilomycin Effect. To explore whether the triple mutants are misfolded proteins recognized by the ERAD (*32*), as previously observed in some ABCG2 mutant proteins (*30*, *33*), we incubated cells overnight separately with either the lysosomal degradation inhibitor, bafilomycin, or the proteasomal degradation inhibitor, MG132, and protein expression levels of the mutants were determined by immunoblotting.

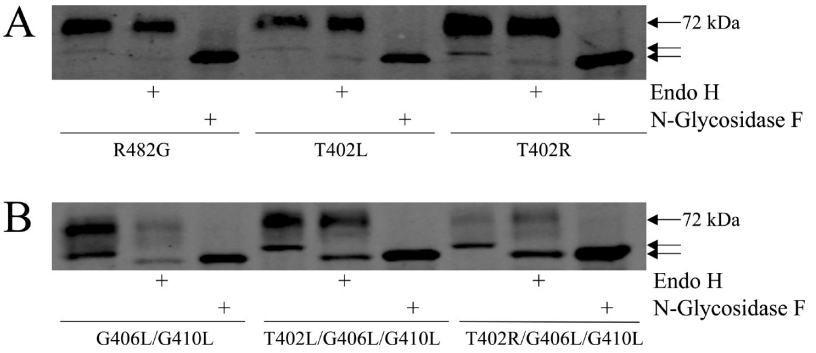

FIGURE 2: Enzymatic deglycosylation with *N*-glycosidase F and Endo H. Immunoblot analysis of cell lysates from the R482G, T402L, and T402R mutants [(A) 35 μg] and from the G406L/G410L, T402L/G406L/G410L, and T402R/G406L/G410L mutants [(B) 70 μg] with the BXP-21 antibody following overnight treatment with Endo H or *N*-glycosidase F. The arrows point out the three different molecular masses observed in the experiment.

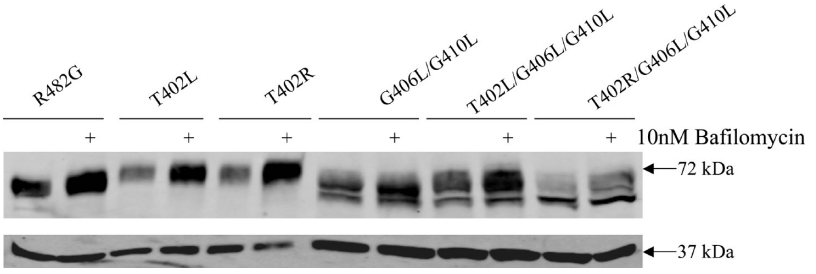

FIGURE 3: Effect of lysosome inhibition on the protein levels of ABCG2 mutants. Cells were harvested after overnight incubation with or without 10 nM bafilomycin followed by immunoblot analysis with the BXP-21 and GAPDH antibodies for the R482G, T402L, and T402R mutants (40 μg/lane) and the G406L/G410L, T402L/G406L/G410L, and T402R/G406L/G410L mutants (100 μg/lane).

Incubation with MG132 did not result in an increased amount of the mutant protein being detected (data not shown). On the other hand, the protein level of the control, T402R, and T402L proteins increased more than 2-fold when cells were treated with bafilomycin, consistent with a previous report that fully processed ABCG2 undergoes lysosomal degradation as part of the protein turnover (*33*). In contrast, the protein levels of the G406L/G410L, T402L/G406L/G410L, and T402R/G406L/G410L mutants were little affected by bafilomycin treatment (Figure 3). This suggests that unlike the wild type, double and triple mutants are likely degraded by an alternate proteosome-independent pathway such as sequestration in aggresomes.

Impact of MX on Localization. In previous studies, treatment with pharmacological chaperones has been reported to improve folding of mutant forms of ABC transporters that are recognized and degraded before maturation in the ER (*34*, *35*). Therefore, we sought to investigate whether the folding of our ABCG2 mutants could be improved via overnight incubation with the ABCG2 substrate MX. Previously, we reported that the levels of the G406L/G410L mutant significantly increased on immunoblot and on immunofluorescence following MX treatment (*19*). In the case of the control, T402L, and T402R proteins, no significant differences between the MX-treated and untreated samples were observed (Figure 4A). As previously shown, a significant increase in protein levels was observed for the G406L/G410L mutant (Figure 4A). In contrast, overnight treatment with MX resulted in a majority of the T402L/G406L/G410L mutant being detected in the normal 72 kDa band as opposed to the double band observed without drug exposure, representing a shift from the lower to the upper molecular mass band (Figure 4A). The average percent of mutant protein detected in the lower and upper bands with and without MX is presented in Figure 4B. Notably, the results obtained with the arginine triple mutant (T402R/G406L/G410L) revealed little shift of the lower band, consistent with a more profound defect.

To further explore the subcellular localization of ABCG2 after MX treatment, the stably transfected HEK cells were examined by immunofluorescence confocal microscopy. No change was observed in the mainly plasma membrane staining for the control, T402L, and T402R proteins after treatment with MX by confocal microscopy (Figure 5). The G406L/G410L mutant exhibited primarily plasma membrane staining with little intracellular signal and after MX treatment displayed a slightly increased level of surface expression. In the case of the T402L/G406L/G410L mutant, both intracellular and cell surface staining could be observed prior to treatment with MX, while after overnight MX treatment, we observed an increased level of ABCG2 plasma membrane localization in the T402L/G406L/G410L mutant (Figure 5). In contrast, after treatment with MX, the T402R/G406L/G410L mutant still primarily displayed intracellular localization.

These results suggest that the higher-molecular mass band visible on immunoblotting following incubation with MX represented the fully mature glycoprotein. To prove this, we performed Endo H digestion on all samples considering that only mutants with altered glycosylation could exhibit sensitivity to Endo H. As demonstrated in Figure 6, following MX treatment, the T402L/G406L/G410L mutant was no longer sensitive to Endo H (Figure 6B), implying that its glycan has matured and that the protein has most likely moved out of the ER. In contrast, the lower-molecular mass form of the T402R/G406L/G410L mutant, which did not shift to the upper 72 kDa band in the presence of MX, was still sensitive to digestion with Endo H (Figure 6B). Interestingly, the lower-molecular mass form of the double mutant also appeared refractory to MX.

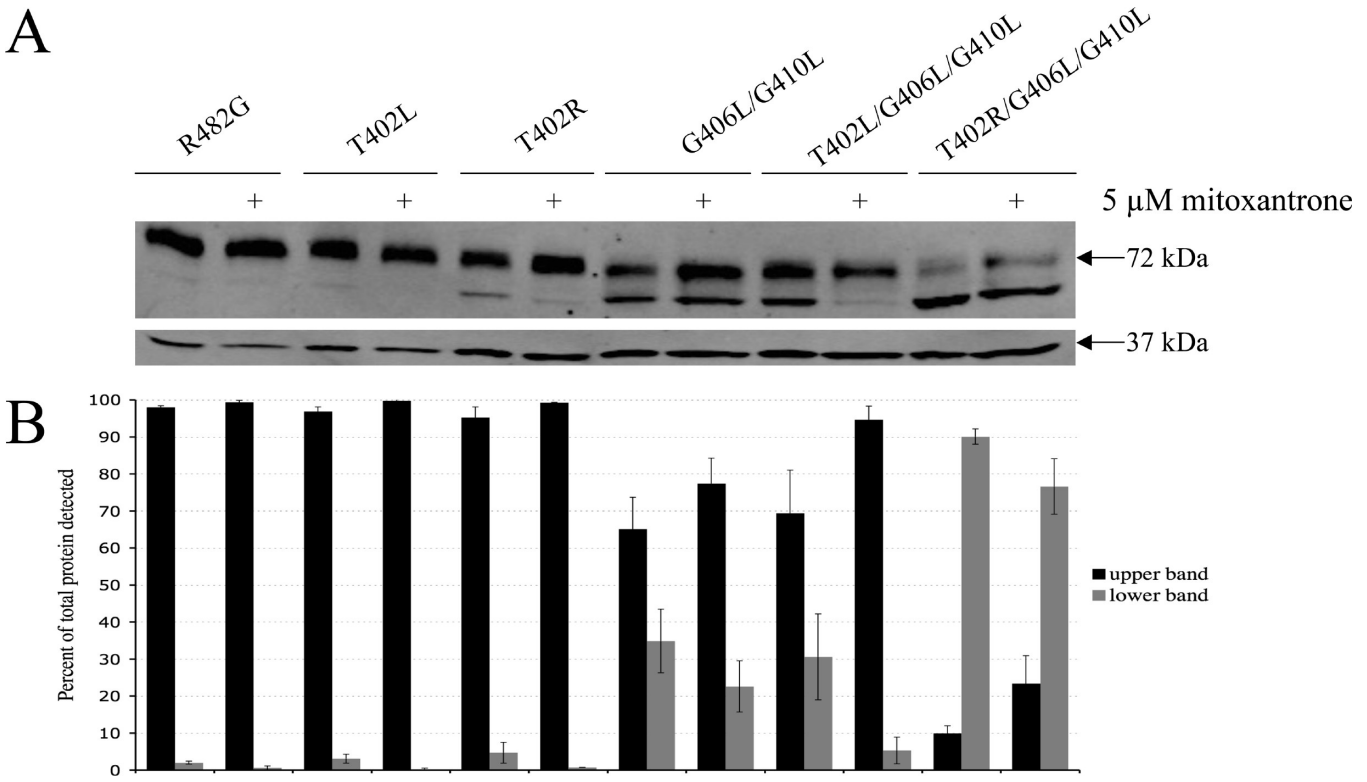

FIGURE 4: "Rescue" of the triple mutants with MX. (A) Following overnight incubation with or without 5 μM MX, cells were harvested, and the lysates (25 μg for R482G, T402R, and T402L and 50 μg for the other mutants) were subjected to immunoblot analysis with the BXP-21 and GAPDH antibodies as described in the legend of Figure 1. (B) Average percent of mutant protein detected in the lower and upper bands with and without MX for at least seven separate experiments.

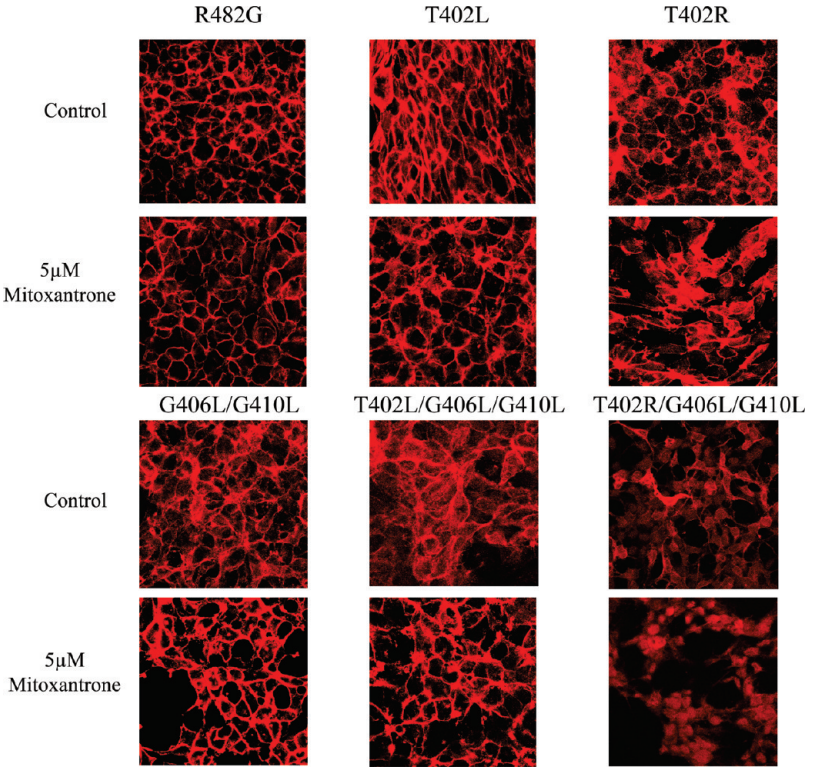

FIGURE 5: Localization of the mutants in HEK 293 cells after treatment with MX. Confocal microscopy of stably transfected HEK 293 after overnight treatment with or without 5 μM MX was performed following fixation with paraformaldehyde and permeabilization with methanol. Immunostaining was conducted for 1 h at room temperature with the BXP-21 monoclonal anti-ABCG2 antibody (red).

Cross-Linking Studies. The results presented so far are consistent with the 402 leucine and particularly arginine mutations combined with the glycine to leucine mutation at the GXXXG motif further destabilizing the ABCG2 dimer. As an indirect way to study dimerization, we performed chemical cross-linking studies. We have previously observed that cross-linking

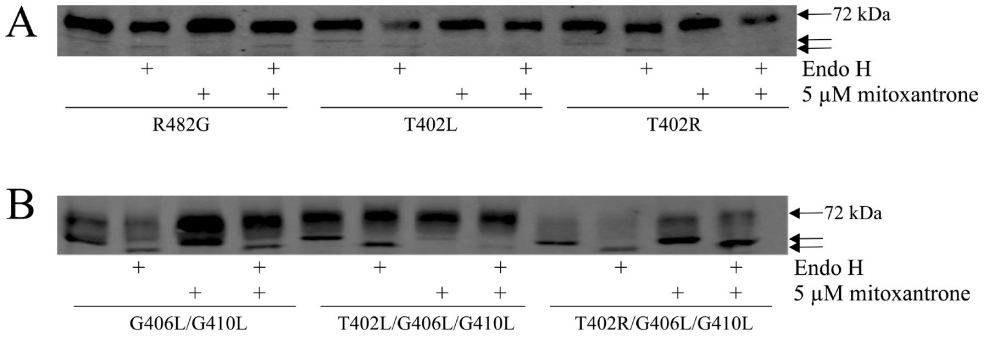

FIGURE 6: Endo H digestion of the triple mutants following MX treatment. After overnight incubation with or without 5 μM MX, cells were harvested, and the lysates were subjected to overnight digestion with Endo H followed by immunoblot analysis with the BXP-21 antibody [(A) 35 μg for R482G, T402R, and T402L and (B) 70 μg for the double and triple mutants].

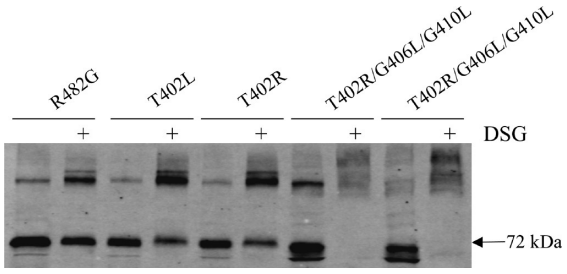

FIGURE 7: Cross-linking studies. Cross-linking was performed on intact cells at room temperature for 30 min with 2 mM DSG followed by protein extraction, SDS−PAGE separation, and immunoblotting with the BXP-21 anti-ABCG2 antibody. Cross-linking is observed in the control, T402L, T402R, and the triple mutants as suggested by higher-molecular mass species. The molecular mass of monomeric wild-type ABCG2 is 72 kDa.

persists in ABCG2 transfectants even when residues predicted to interfere with dimerization are disrupted (*24*) and evaluated in this context. HEK 293 cells transfected with the mutants were treated with the amine reactive cross-linker DSG, followed by protein extraction and immunoblot analysis with the BXP-21 antibody. Figure 7 demonstrates increased molecular mass bands consistent with cross-linking of the control, T402R, and T402R/G406L/G410L proteins. Similar results were obtained with the T402L and T402L/G406L/G410L mutants with DSG; furthermore, the triple mutants were also cross-linked by DSS at both 4 °C and room temperature (data not shown).

TOXCAT Assay. As another approach to assessing the possible impact of the extended TXXXGXXXG motif on dimerization or interhelical packing, we performed the so-called TOXCAT assay using peptides corresponding to TM1 of ABCG2 (*25*). This assay uses chimeric constructs expressed in MalE deficient/*E. coli*/NT326, which, being bacteria, lack ERAD, and the construct ensures proper expression in the cytoplasmic membrane. The constructs are composed of the TM of interest connected to the DNA binding domain of the dimerization-dependent transcriptional activator ToxR at one end and to the maltose binding protein at the other end, the latter ensuring correct orientation in the membrane. If dimerization of the TMs occurs, two ToxR molecules also form a dimer and mediate transcription of the CAT gene and subsequent resistance to chloramphenicol (Figure 8A). To evaluate the extended TXXXGXXXG motif in ABCG2, we substituted threonine 402 with arginine, since it had a greater impact on the protein relative to leucine (as suggested by the differences observed in localization and ability to be rescued by MX).

Figure 8B shows that the TM carrying the T402R mutation had CAT activity comparable to that of wild-type ABCG2 TM1. In contrast, G406L/G410L and T402R/G406L/G410L demonstrated an approximately 50% or more decrease in their CAT activity, implying impaired dimerization of these mutant TMs. While the helical partner for TM1 in intact ABCG2 is not thought to be TM1 of the opposite ABCG2 molecule (see below), in the TOXCAT assay, the only possible partner is another TM1 segment. Thus, this assay primarily tests the ability of the TM to undergo tight intrahelical packing.

Structural Model. To look at the possible role of T402 in ABCG2 dimerization, we performed a molecular modeling study. To do this, we constructed an ABCG2 atomic model using the crystal structure of a bacterial ABC half-transporter Sav1866 as a modeling template for the TMD and that of *E. coli* MalK for the NBD. The model was verified on the basis of existing biochemical and mutational data available for ABCG2 as well as structural data for membrane proteins in general and for ABC transporters in particular. Although the model was entirely constructed considering the sequence alignment and without prior knowledge of the T402 mutations, it nevertheless places the TXXXGXXXG motif of TM1 at the dimer interface facing TM6 of the adjacent subunit (Figure 9A,B). In the model, the GXXXG motif makes contact with the hydrophobic surface of TM6 intimately, whereas the side chain of T402 faces potentially the side chains of Met636 and I637 in TM6 and that of V556 from TM5. The side chain of T402 appears to have much leeway and points to a large cavity created by a slight turn of the TM1 helix at this position (Figure 9A−C). When created in silico, the T402L mutation does not appear to interfere with interhelix packing between TM1 and TM5 and TM6 of its adjacent subunit (Figure 9D), which is consistent with the biochemical data for this mutant. Likewise, any interference by the longer side chain of the arginine mutant may be alleviated due to the unique position of T402 in TM1 (Figure 9E).

DISCUSSION

We have been interested in identifying residues critical to the dimerization of ABCG2. We initially studied a GXXXG motif homologous to the dimerization motif in glycophorin A, mutating glycines to leucines in TM1 of ABCG2 transfected in HEK 293 cells. We demonstrated cell surface expression and intact cross-linking, but a lack of function in the mutants, and concluded that the results were consistent but not proof of a role for the GXXXG motif in dimerization (*19*). In the study presented here, we examined the role of threonine 402, located

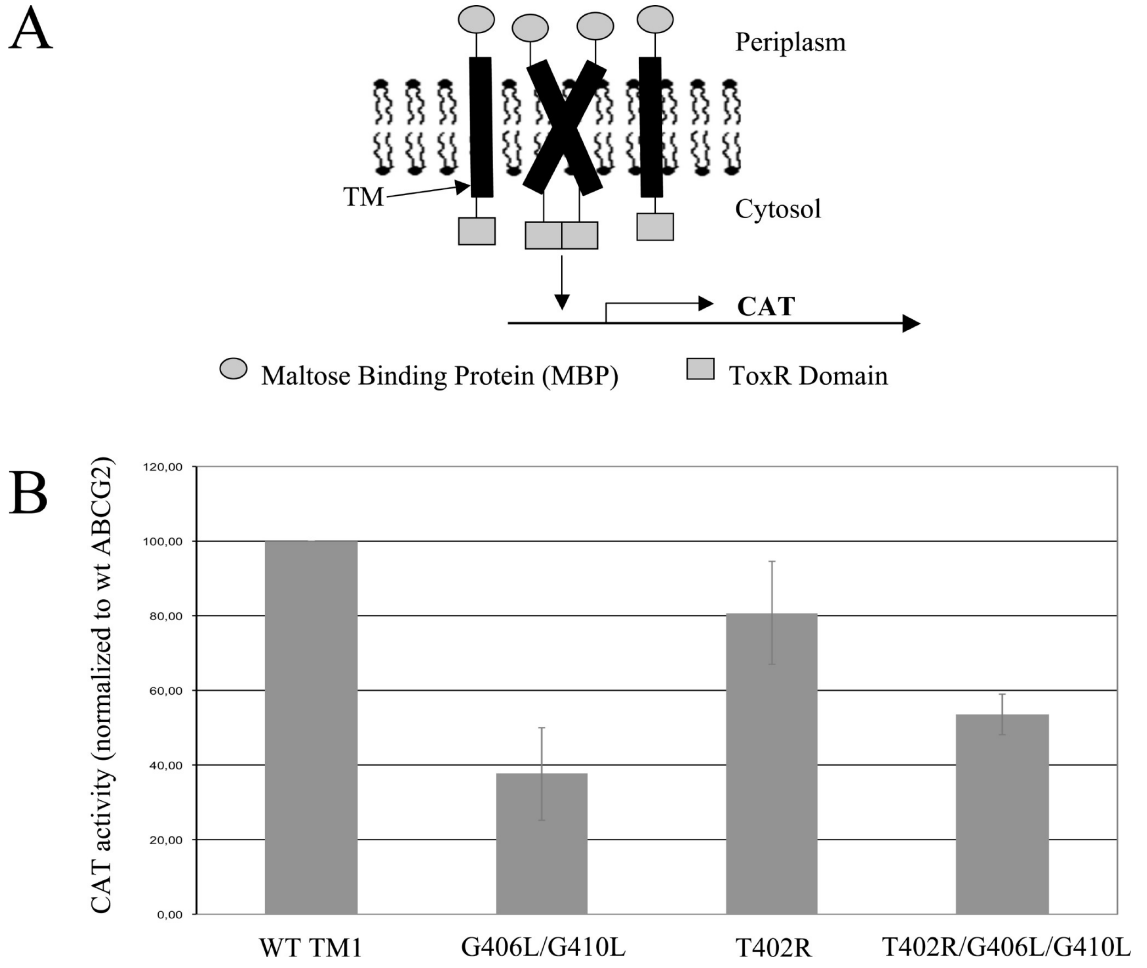

FIGURE 8: TOXCAT assay. (A) Schematic representation of the assay. TM α-helices are fused with the ToxR domain on one end and with the maltose binding protein on the other. If dimerization of the TMs occurs, ToxR forms an active dimer and CAT is transcribed. (B) CAT activity measured in the TOXCAT assay for the G406L/G410L, T402R, and T402R/G406L/G410L mutants compared to that of wild-type TM1 of ABCG2.

three residues from the GXXXG motif of TM1. Mutating T402 alone did not result in a significant change from the wild-type phenotype. However, T402 mutations in addition to mutations in the GXXXG motif caused a reduction in the level of protein expression and drug efflux, alterations in glycosylation, and retention in the ER. Following incubation with the ABCG2 substrate, MX, T402L/T406L/T410L readily shifted to the plasma membrane while T402R/T406L/T410L did not. TOXCAT and molecular modeling of ABCG2 were used to further explore the role of T402 in dimerization.

Dimerization may occur at various stages in protein biosynthesis. A common mechanism, observed in proteins such as EGFR, AhR, GCR, and SRC, involves ligand binding-induced receptor dimerization at the cell surface (*36*). In contrast to this system of dimerization, ABCG2 dimerizes at an earlier stage of processing at the ER. This sequence is shared by GPCRs where, as similarly hypothesized for ABCG2, dimerization at the ER plays an important role in the quality-control system (*37*). An example similar to ABCG2 can be found in ABC half-transporters ABCG5 and ABCG8 which are obligate heterodimers that are thought to dimerize in the ER and then exit the ER together and travel through the Golgi for post-translational modification before reaching the apical plasma membrane (*38*, *39*).

In glycophorin A, threonine 87 is the only polar amino acid in the seven-residue dimerization motif. Mutating this threonine to valine in glycophorin A results in partial destabilization of the homodimer. The impact of this mutation, which replaces the Thr87 γ-hydroxyl group with a methyl group of roughly the same molecular volume, suggests that the threonine residue stabilizes the dimer via formation of a hydrogen bond (*22*, *38*, *40*−*44*). When analyzing 11 transmembrane protein structures, Senes et al. (*45*) found parallel right handed α-helices to be rich in glycine, serine, and threonine with clusters of Cα−H···O contacts as common features. Small residues like glycine and serine allow close packing of helices and facilitate formation of hydrogen bonds. Threonine residues frequently form interhelical Cα−H···O bonds and are one of the most common polar residues in TMs.

Under the consideration that the GXXXG motif in TM1 may be involved in the dimer interface, or alternatively, in a transient interaction with the TM1 of a neighboring subunit, we chose to substitute threonine with leucine at position 402 in the mammalian system to replace a polar with a nonpolar residue, similar to the substitution disruptive of Thr87 with Val in glycophorin A (*22*), and in doing so also introduced a small increase in size. In glycophorin A, the rank of disruption for mutation at position Thr87 is correlated with size (Ala < Val < Ile < Leu) (*46*). More importantly, we wanted to use the T402L substitution to probe the existence of the perceived hydrogen bonding interaction by T402. The wild-type phenotype of the T402L mutant argues against H-bonding at this residue. Indeed, molecular modeling places T402 opposite I637 in TM6 from its dimeric partner.

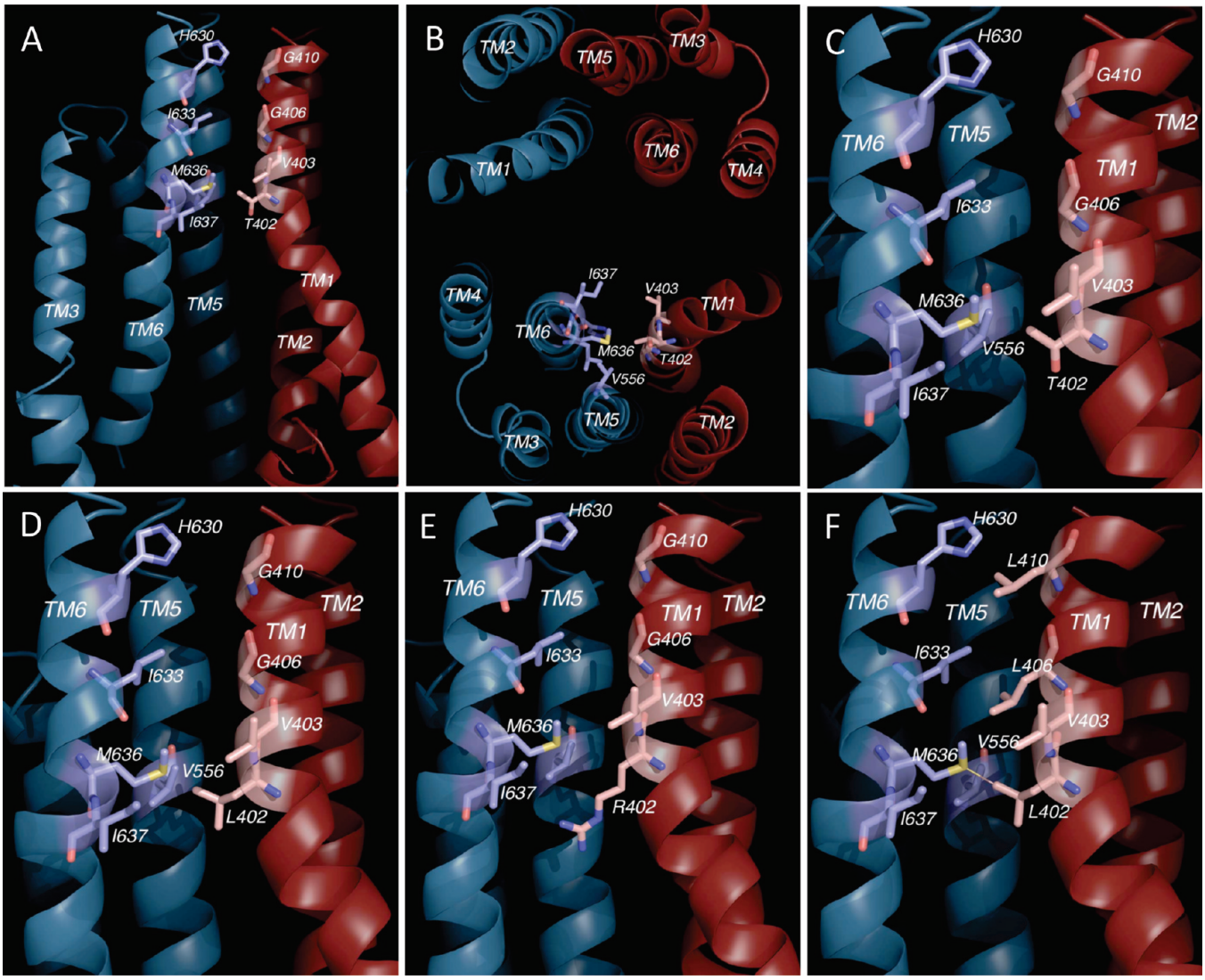

FIGURE 9: Homology modeling of ABCG2. (A) Cross section of the ABCG2 homology model showing the TXXXGXXXG motif and its vicinity, including TM1 and TM2 from one subunit (dark red) and TM3, TM5, and TM6 from another (dark blue). A putative drug-binding cavity below T402 is also illustrated. (B) View of the TMD of the ABCG2 model along the direction perpendicular to the membrane plane showing the arrangement of 12 TM helices and the position of the TXXXGXXXG motif. (C) Close-up view of the wild-type TXXXGXXXG motif. (D) Close-up view of the T402L mutation. (E) Close-up view of the T402R mutation. (F) Close-up view of the T402L, G406L, and G410L mutations.

Further, the leucine substitution at 402 may potentially interact more favorably with I637 of its dimeric partner than the threonine residue and actually promote dimer formation. This point is supported by the efficient shift of the lower band in the MX rescue experiments for the T402L and T402L/G406L/G410L mutants discussed below. Although the substitution with the larger positively charged arginine was expected to be an unfavorable change in the membrane environment and likely to disrupt the association of the transmembrane helices, the T402R mutant appeared on the cell surface and is capable of efflux. It should be noted that the level of disruption in a TM due to an arginine is highly dependent on location. The effect can range from disruption to no effect to improved folding, as observed in arginine scanning mutagenesis of the transmembrane helix of P-glycoprotein (*47*). Molecular modeling places T402 at a position where the side chain of T402 has more room to maneuver, possibly protrudes into the substrate-binding pocket, and thus is capable of accommodating large residue changes (Figure 9).

Our results with the ABCG2 triple mutants carrying the threonine 402 to leucine or arginine substitutions (T402R/G406L/G410L and T402R/G406L/G410L) are consistent with destabilization of the homodimer. Since we did not observe a major disruption with either substitution at position 402 alone, we can conclude that the entire TXXXGXXXG motif is important in ABCG2. Our previous studies of ABCG2 dimerization have suggested a dynamic process that happens as the monomers are synthesized and fold together in the ER. Our immunostaining and enzymatic deglycosylation studies indicate that both triple mutants, the arginine substitution more than the leucine substitution, demonstrated retention in the ER, suggesting that the mutants are most likely recognized by the ERAD as misfolded proteins. Although the data suggest ERAD-mediated degradation, in the case of our mutants, proteasomal inhibition with MG132 did not result in an increased amount of the mutant proteins detected (data not shown), suggesting clearance of the proteins through an alternative mechanism such as sequestration in aggresomes. Notably, despite retention in the ER and altered glycosylation, the mutant proteins could be cross-linked with DSG and DSS. This is consistent with our previous results in which cross-linking occurred no matter how significant the

mutation (*24*, *30*). We have thus concluded that positive results obtained in cross-linking experiments do not differentiate between proximity in the ER during protein synthesis and the formation of a proper dimer that can translocate to the cell surface.

Treatment with pharmacological chaperones has been shown to promote folding and cellular expression of GPCRs when mutant forms retained in the ER are studied (*48*). Lipophilic β-adrenergic ligands such as pharmacological chaperones were able to restore dimerization and membrane expression of the homodimerization-compromised β1-adrenoceptor mutants retained in the ER (*49*). Rescuing misfolded membrane proteins with pharmacological chaperones is an intensively studied strategy in certain disease-causing mutations (*34*, *35*). One particularly relevant example is the ABC transporter cystic fibrosis transmembrane conductance regulator (CFTR), in which, interestingly, less than 50% of even the wild-type protein is folded correctly (*50*). Mutations causing cystic fibrosis disrupt folding, and some mutants are completely retained in the ER. These proteins can be rescued to some extent by pharmacological chaperones such as doxorubicin (*51*) and sildenafil (*52*). We previously noted that only a small portion of wild-type ABCG2 is likely misfolded (*30*). As noted above, the T402L/G406L/G410L mutant could be rescued by overnight treatment with the substrate MX as suggested by its shift to the normal 72 kDa molecular mass band on immunoblot and its loss of Endo H sensitivity. Indeed, the substitution of leucine at 402 may have provided a slight benefit in protein stability in the presence of the pharmacological chaperone as evidenced by the better shift of the lower-molecular mass band relative to that of the double mutant alone. In contrast, the T402R/G406L/G410L mutant, carrying the more drastic substitution at residue 402, did not show the same phenomenon (Figures 4−6).

The studies presented here are consistent with but do not conclusively show a role for the GXXXG motif in ABCG2 dimerization. Other roles for the GXXXG motif include involvement in higher-order oligomerization as noted above, given that tetramers and even higher-order oligomers of ABCG2 have been described as forming the functional transporter (*53*, *54*). Other possibilities include interhelical packing within the monomer or a transient role in a folding intermediate of the protein. Considering the GXXXG motif in TM1 of ABCG2 important in any one of the processes mentioned above, mutations could equally result in aberrant folding and activation of the ERAD as noted above. To evaluate these possibilities, we utilized the TOXCAT assay, which allows investigation of single transmembrane helix associations in biological membranes (*25*). The level of CAT activity measured in the TOXCAT assay indicates the strength of TM association. The results with the wild type do confirm that ABCG2 TM1 is able to self-associate when expressed in bacterial cells. The level of this dimerization is significantly reduced via alteration of the TXXXGXXXG motif, confirming the latter's importance. Whether this self-association could reflect a role for ABCG2 TM1 forms in dimerization or a higher-order oligomerization such as the tetrameric structure reported in protein purification systems is a matter for future study (*53*, *54*).

In conclusion, we have observed that mutating threonine 402 to either leucine or arginine in addition to the leucine substitutions at the GXXXG motif in TM1 of ABCG2 further destabilized the protein, resulting in mutants that not only were impaired in their function but also were partially retained in the ER. The arginine substitution rendered the protein insensitive to pharmacological rescue. The data presented suggest that the ABCG2 homodimer folds together in the ER and that the drug binding sites are accessible enough for MX to bind and act as a pharmacologic chaperone improving protein processing. The studies echo those of Loo and Clark (*35*), who have shown that pharmacologic chaperones are able to increase levels of a functional transporter on the cell surface. The ability of chemical cross-linking agents to cross-link ABCG2 despite its failure to form a functional dimer suggests one of two possibilities: two loosely folded monomers associate and rearrange to form a functional dimer and failing that are recognized by ERAD, or two ribosomes simultaneously produce the monomers which fold together in the ER. The data suggest that homodimerization occurs early in the biosynthetic process in the ER and that conformational changes imposed by the mutations could independently affect dimerization and cell surface trafficking (*49*).

ACKNOWLEDGMENT

We thank Drs. Tito Fojo and Ramanujan Hegde for their valuable advice.

REFERENCES

1. Dean, M., Hamon, Y., and Chimini, G. (2001) The human ATP-binding cassette (ABC) transporter superfamily. *J. Lipid Res. 42*, 1007–1017.
2. Allikmets, R., Schriml, L. M., Hutchinson, A., Romano-Spica, V., and Dean, M. (1998) A human placenta-specific ATP-binding cassette gene (ABCP) on chromosome 4q22 that is involved in multidrug resistance. *Cancer Res. 58*, 5337–5339.
3. Miyake, K., Mickley, L., Litman, T., Zhan, Z., Robey, R., Cristensen, B., Brangi, M., Greenberger, L., Dean, M., Fojo, T., and Bates, S. E. (1999) Molecular cloning of cDNAs which are highly overexpressed in mitoxantrone-resistant cells: Demonstration of homology to ABC transport genes. *Cancer Res. 59*, 8–13.
4. Doyle, L. A., Yang, W., Abruzzo, L. V., Krogmann, T., Gao, Y., Rishi, A. K., and Ross, D. D. (1998) A multidrug resistance transporter from human MCF-7 breast cancer cells. *Proc. Natl. Acad. Sci. U.S.A. 95*, 15665–15670.
5. Chen, Z. S., Robey, R. W., Belinsky, M. G., Shchaveleva, I., Ren, X. Q., Sugimoto, Y., Ross, D. D., Bates, S. E., and Kruh, G. D. (2003) Transport of methotrexate, methotrexate polyglutamates, and 17β-estradiol 17-(β-D-glucuronide) by ABCG2: Effects of acquired mutations at R482 on methotrexate transport. *Cancer Res. 63*, 4048–4054.
6. Maliepaard, M., van Gastelen, M. A., de Jong, L. A., Pluim, D., van Waardenburg, R. C., Ruevekamp-Helmers, M. C., Floot, B. G., and Schellens, J. H. (1999) Overexpression of the BCRP/MXR/ABCP gene in a topotecan-selected ovarian tumor cell line. *Cancer Res. 59*, 4559–4563.
7. Kawabata, S., Oka, M., Shiozawa, K., Tsukamoto, K., Nakatomi, K., Soda, H., Fukuda, M., Ikegami, Y., Sugahara, K., Yamada, Y., Kamihira, S., Doyle, L. A., Ross, D. D., and Kohno, S. (2001) Breast cancer resistance protein directly confers SN-38 resistance of lung cancer cells. *Biochem. Biophys. Res. Commun. 280*, 1216–1223.
8. Robey, R. W., Medina-Perez, W. Y., Nishiyama, K., Lahusen, T., Miyake, K., Litman, T., Senderowicz, A. M., Ross, D. D., and Bates, S. E. (2001) Overexpression of the ATP-binding cassette half-transporter, ABCG2 (MXR/BCRP/ABCP1), in flavopiridol-resistant human breast cancer cells. *Clin. Cancer Res. 7*, 145–152.
9. Polgar, O., Robey, R. W., and Bates, S. E. (2008) ABCG2: Structure, function and role in drug response. *Expert Opin. Drug Metab. Toxicol. 4*, 1–15.
10. Robey, R. W., To, K. K., Polgar, O., Dohse, M., Fetsch, P., Dean, M., and Bates, S. E. (2009) ABCG2: A perspective. *Adv. Drug Delivery Rev. 61*, 3–13.
11. Cusatis, G., and Sparreboom, A. (2008) Pharmacogenomic importance of ABCG2. *Pharmacogenomics 9*, 1005–1009.
12. Zhou, S., Morris, J. J., Barnes, Y., Lan, L., Schuetz, J. D., and Sorrentino, B. P. (2002) Bcrp1 gene expression is required for normal numbers of side population stem cells in mice, and confers relative protection to mitoxantrone in hematopoietic cells in vivo. *Proc. Natl. Acad. Sci. U.S.A. 99*, 12339–12344.
13. Henriksen, U., Fog, J. U., Litman, T., and Gether, U. (2005) Identification of intra- and intermolecular disulfide bridges in the multidrug resistance transporter ABCG2. *J. Biol. Chem. 280*, 36926–36934.

14. Kage, K., Fujita, T., and Sugimoto, Y. (2005) Role of Cys-603 in dimer/oligomer formation of the breast cancer resistance protein BCRP/ABCG2. *Cancer Sci. 96*, 866–872.
15. Wakabayashi, K., Nakagawa, H., Adachi, T., Kii, I., Kobatake, E., Kudo, A., and Ishikawa, T. (2006) Identification of cysteine residues critically involved in homodimer formation and protein expression of human ATP-binding cassette transporter ABCG2: A new approach using the flp recombinase system. *J. Exp. Ther. Oncol. 5*, 205–222.
16. Liu, Y., Yang, Y., Qi, J., Peng, H., and Zhang, J. T. (2008) Effect of cysteine mutagenesis on the function and disulfide bond formation of human ABCG2. *J. Pharmacol. Exp. Ther. 326*, 33–40.
17. Poelarends, G. J., and Konings, W. N. (2002) The transmembrane domains of the ABC multidrug transporter LmrA form a cytoplasmic exposed, aqueous chamber within the membrane. *J. Biol. Chem. 277*, 42891–42898.
18. Heintke, S., Chen, M., Ritz, U., Lankat-Buttgereit, B., Koch, J., Abele, R., Seliger, B., and Tampe, R. (2003) Functional cysteine-less subunits of the transporter associated with antigen processing (TAP1 and TAP2) by de novo gene assembly. *FEBS Lett. 533*, 42–46.
19. Polgar, O., Robey, R. W., Morisaki, K., Dean, M., Michejda, C., Sauna, Z. E., Ambudkar, S. V., Tarasova, N., and Bates, S. E. (2004) Mutational analysis of ABCG2: Role of the GXXXG motif. *Biochemistry 43*, 9448–9456.
20. Russ, W. P., and Engelman, D. M. (2000) The GxxxG motif: A framework for transmembrane helix-helix association. *J. Mol. Biol. 296*, 911–919.
21. Brosig, B., and Langosch, D. (1998) The dimerization motif of the glycophorin A transmembrane segment in membranes: Importance of glycine residues. *Protein Sci. 7*, 1052–1056.
22. Lemmon, M. A., Flanagan, J. M., Treutlein, H. R., Zhang, J., and Engelman, D. M. (1992) Sequence specificity in the dimerization of transmembrane α-helices. *Biochemistry 31*, 12719–12725.
23. Honjo, Y., Hrycyna, C. A., Yan, Q. W., Medina-Perez, W. Y., Robey, R. W., van de Laar, A., Litman, T., Dean, M., and Bates, S. E. (2001) Acquired mutations in the MXR/BCRP/ABCP gene alter substrate specificity in MXR/BCRP/ABCP-overexpressing cells. *Cancer Res. 61*, 6635–6639.
24. Polgar, O., Ozvegy-Laczka, C., Robey, R. W., Morisaki, K., Okada, M., Tamaki, A., Koblos, G., Elkind, N. B., Ward, Y., Dean, M., Sarkadi, B., and Bates, S. E. (2006) Mutational Studies of G553 in TM5 of ABCG2: A Residue Potentially Involved in Dimerization. *Biochemistry 45*, 5251–5260.
25. Russ, W. P., and Engelman, D. M. (1999) TOXCAT: A measure of transmembrane helix association in a biological membrane. *Proc. Natl. Acad. Sci. U.S.A. 96*, 863–868.
26. Li, Y., Polgar, O., Okada, M., Esser, L., Bates, S., and Xia, D. (2006) Towards understanding the mechanism of action of the multidrug resistance-linked half-ABC transporter ABCG2: A molecular modeling study. *J. Mol. Graphics Modell. 25*, 837–851.
27. Adamian, L., and Liang, J. (2006) Prediction of transmembrane helix orientation in polytopic membrane proteins. *BMC Struct. Biol. 6*, 13.
28. Dawson, R. J., and Locher, K. P. (2006) Structure of a bacterial multidrug ABC transporter. *Nature 443*, 180–185.
29. Chen, J., Lu, G., Lin, J., Davodson, A. L., and Quiocho, F. A. (2003) A tweezers-like motion of the ATP-binding cassette dimer in an ABC transport cycle. *Mol. Cell 12*, 651–661.
30. Polgar, O., Ediriwickrema, L. S., Robey, R. W., Sharma, A., Hegde, R. S., Li, Y., Xia, D., Ward, Y., Dean, M., Ozvegy-Laczka, C., Sarkadi, B., and Bates, S. E. (2009) Arginine 383 is a crucial residue in ABCG2 biogenesis. *Biochim. Biophys. Acta 1788*, 1434–1443.
31. Diop, N. K., and Hrycyna, C. A. (2005) N-Linked glycosylation of the human ABC transporter ABCG2 on asparagine 596 is not essential for expression, transport activity, or trafficking to the plasma membrane. *Biochemistry 44*, 5420–5429.
32. Wakabayashi-Nakao, K., Tamura, A., Furukawa, T., Nakagawa, H., and Ishikawa, T. (2009) Quality control of human ABCG2 protein in the endoplasmatic reticulum: Ubiquitination and proteosomal degradation. *Adv. Drug Delivery Rev. 61*, 66–72.
33. Furukawa, T., Wakabayashi, K., Tamura, A., Nakagava, H., Morishima, Y., Osawa, Y., and Ishikawa, T. (2009) Major SNP (Q141K) variant of human ABC transporter ABCG2 undergoes lysosomal and proteasomal degradations. *Pharm. Res. 26*, 469–479.
34. Loo, T. W., and Clarke, D. M. (2007) Chemical and pharmacological chaperones as new therapeutic agents. *Expert Rev. Mol. Med. 9*, 1–18.
35. Loo, T. W., Bartlett, M. C., and Clarke, D. M. (2005) Rescue of folding defects in ABC transporters using pharmacological chaperones. *J. Bioenerg. Biomembr. 37*, 501–507.
36. Schlessinger, J. (2002) Ligand-Induced, Receptor-Mediated Dimerization and Activation of EGF Receptor. *Cell 110*, 669–672.
37. Terrillon, S., and Bouvier, M. (2003) Roles of G-protein-coupled receptor dimerization. *EMBO Rep. 5*, 30–34.
38. Graf, G. A., Yu, L., Li, W. P., Gerard, R., Tuma, P. L., Cohen, J. C., and Hobbs, H. H. (2003) ABCG5 and ABCG8 are obligate heterodimers for protein trafficking and biliary cholesterol excretion. *J. Biol. Chem. 278*, 48275–48282.
39. Graf, G. A., Li, W. P., Gerard, R. D., Gelissen, I., White, A., Cohen, J. C., and Hobbs, H. H. (2002) Coexpression of ATP-binding cassette proteins ABCG5 and ABCG8 permits their transport to the apical surface. *J. Clin. Invest. 110*, 659–669.
40. Hildebrand, P. W., Gunther, S., Goede, A., Forrest, L., Frommel, C., and Preissner, R. (2008) Hydrogen-bonding and packing features of membrane proteins: Functional implications. *Biophys. J. 94*, 1945–1953.
41. Smith, S. O., Song, D., Shekar, S., Groesbeek, M., Ziliox, M., and Aimoto, S. (2001) Structure of the transmembrane dimer interface of glycophorin A in membrane bilayers. *Biochemistry 40*, 6553–6558.
42. Smith, S. O., Eilers, M., Song, D., Crocker, E., Ying, W., Groesbeek, M., Metz, G., Ziliox, M., and Aimoto, S. (2002) Implications of threonine hydrogen bonding in the glycophorin A transmembrane helix dimer. *Biophys. J. 82*, 2476–2486.
43. MacKenzie, K. R., Prestegard, J. H., and Engelman, D. M. (1997) A transmembrane helix dimer: Structure and implications. *Science 276*, 131–133.
44. Cuthbertson, J. M., Bond, P. J., and Sansom, M. S. (2006) Transmembrane helix-helix interactions: Comparative simulations of the glycophorin a dimer. *Biochemistry 45*, 14298–14310.
45. Senes, A., Ubarretxena-Belandia, I., and Engelman, D. M. (2001) The Cα−H···O hydrogen bond: A determinant of stability and specificity in transmembrane helix interactions. *Proc. Natl. Acad. Sci. U.S.A. 98*, 9056–9061.
46. Duong, M. T., Jaszewki, T. M., Fleming, K. G., and MacKenzie, K. R. (2007) Changes in apparent free energy of helix-helix dimerization in a biological membrane due to point mutations. *J. Mol. Biol. 371*, 422–434.
47. Loo, T. W., Bartlett, M. C., and Clarke, D. M. (2009) Identification of residues in the drug translocation pathway of the human multidrug resistance P-glycoprotein by arginine mutagenesis. *J. Biol. Chem. 284*, 24074–24087.
48. Bernier, V., Bichet, D. G., and Bouvier, M. (2004) Pharmacological chaperone action on G-protein-coupled receptors. *Curr. Opin. Pharmacol. 4*, 520–533.
49. Kobayashi, H., Ogawa, K., Yao, R., Lichtarge, O., and Bouvier, M. (2009) Functional Rescue of β1-Adrenoceptor Dimerization and Trafficking by Pharmacological Chaperones. *Traffic 10*, 1019–1033.
50. Ward, C. L., and Kopito, R. R. (1994) Intracellular turnover of cystic fibrosis transmembrane conductance regulator. Inefficient processing and rapid degradation of wild-type and mutant proteins. *J. Biol. Chem. 269*, 25710–25718.
51. Maitra, R., Shaw, C. M., Stanton, B. A., and Hamilton, J. W. (2001) Increased functional cell surface expression of CFTR and ΔF508-CFTR by the anthracycline doxorubicin. *Am. J. Physiol. 280*, C1031–C1037.
52. Dormer, R. L., Harris, C. M., Clark, Z., Pereira, M. M., Doull, I. J., Norez, C., Becq, F., and McPherson, M. A. (2005) Sildenafil (Viagra) corrects ΔF508-CFTR location in nasal epithelial cells from patients with cystic fibrosis. *Thorax 60*, 55–59.
53. McDevitt, C. A., Collins, R. F., Conway, M., Modok, S., Storm, J., Kerr, I. D., Ford, R. C., and Callaghan, R. (2006) Purification and 3D structural analysis of oligomeric human multidrug transporter ABCG2. *Structure 14*, 1623–1632.
54. Xu, J., Liu, Y., Yang, Y., Bates, S., and Zhang, J. T. (2004) Characterization of oligomeric human half-ABC transporter ATP-binding cassette G2. *J. Biol. Chem. 279*, 19781–19789.